

Full Length Research Paper

Amplitude versus offset (AVO) analysis modelling in hydrocarbon exploration: A case study

Züheyr Kamacı* and Canan Çiftçi

Department of Geophysics Engineering, Faculty of Engineering and Architecture, Suleyman Demirel University, Isparta 32260, Turkey.

Accepted 15 February, 2011

In this study, the geological model used for amplitude versus offset (AVO) analysis, was created by synthetic well logs. The geological model is comprised of shale, gassy-sand, clay and sand layers. The synthetic seismic records including 230 shooting and 60 folds were constructed over the model. The data processing has been applied to the synthetic records. After the data processing, AVO analysis has been applied to synthetic data. Class III AVO anomaly has been obtained from the common depth point gathers. Also intercept, gradient, intercept* gradient and cross-plot attributes had been calculated. Analysis has shown that the amplitude increases with increasing offset. The gassy sand anomalies were also obtained by the AVO attributes. In addition, the advantages and disadvantages of AVO analysis were discussed in this study.

Key words: Geological model, reflection amplitude, reflection angle, hydrocarbon rock physics, amplitude versus offset attributes.

INTRODUCTION

The seismic reflection method used in hydrocarbon exploration is rather expensive and risky method compared with the other geophysical methods. A petroleum well which has insufficient reserve is a waste of time and lost of money for the petroleum explorations. Therefore, in seismic studies the amplitude versus offset (AVO) analysis is widely applied with other data processing techniques in order to reduce the risk on interpretation. Recently, benefiting from the seismic reflection characteristics the AVO analysis as a seismic tool has been applied in several studies so as to decrease the risk. Furthermore, the AVO technique is used to model the subsurface structures and as a direct technique to identify the natural gas reservoirs. In addition, the results of AVO analysis are used to easily predict the seismic parameters derived from bottom simulating reflector (BSR) through forward modelling

approach (Yavuz and Demirbağ, 2010). Also, it has been shown that the amplitude versus angle (AVA) and Lambda-Mu-Rho (LMR) analysis techniques can be used as seismic attributes for identification and determination of the fluid type including gas, water and solved gases in the reservoir rocks (Sandıkçı, 2010).

AVO analysis as a seismic exploration tool investigates the dependence of seismic reflection amplitudes on the offset distance. The dependence of seismic energy at an interface on the reflection coefficients, incidence angle and the elastic parameters of the medium was firstly studied by Knott (1899) and then the subject was introduced to the geophysicists by Zoeppritz (1919). Since the solution of the Zoeppritz matrix equations including several unknowns require large computation times the researches such as Bortfeld (1961), Richards and Frasier (1976), Aki and Richards (1980) and Shuey (1985) neglecting some of the parameters in the equations and making some assumptions obtained an approximate solution.

Basically, the AVO method requires three principle applications. Firstly, analysis and interpretation of seismic

*Corresponding author. E-mail: zuheyrkamaci@gmail.com.
Tel: +90 246 211 13 57. Fax: +90 246 237 08 59.

data named as AVO detection, secondly, sustaining the result obtained from the assessment of seismic data through modelling named as AVO modelling, and, thirdly, a lithological characterization named as inversion of AVO data (Sincer, 2008).

Several seismic data processing stages need to be performed before AVO analysis is applied. The data processing stages depends on the data itself. Ostrander (1984), Chiburis (1984), Yu (1985) and Todd (1986) suggested several data processing tools for some particular purposes. During the AVO analysis it is important not to distort the true amplitudes varying with the offset distances.

In the present study, the synthetic seismic reflection data were obtained from the shots on a geological model comprised of shale, gassy sand and clay-sand layers. Following general seismic data processing stages, AVO analysis was applied. Moreover, intercept, gradient, intercept* gradient and cross-plot AVO attributes had been calculated. Analysis has shown that the amplitude increases with increasing offset. The gassy sand anomalies were also obtained by the AVO attributes (Çiftçi, 2008; Çiftçi et al., 2009).

MATERIALS AND METHODS

The modelling given in the present study was carried out in the Data Processing Center of TPAO (Turkish Petroleum Corporation) using the ProMax software. The Shuey (1985) approach explained below was used for the model development. The advantage of this approach is that each term defines the angle spacing in the offset curve.

$$R_{pp}(\theta_1) \approx R_p + \left(A_0 R_p + \frac{\Delta\sigma}{(1-\sigma)^2} \right) \sin^2 \theta_1 + \frac{1}{2} \frac{\Delta Vp}{Vp_a} (\tan^2 \theta_1 - \sin^2 \theta_1) \quad (1)$$

$$A_0 = B_0 - 2(1 + B_0) * \left(\frac{1 - 2\sigma}{1 - \sigma} \right) \quad (2)$$

$$B_0 = \frac{\frac{\Delta Vp}{Vp_a}}{\frac{\Delta Vp}{\Delta Vp_a} + \frac{\Delta\rho}{\Delta\rho_a}} \quad (3)$$

$$R_{pp}(\theta_1) \approx R_p + B \sin^2 \theta_1 + C(\tan^2 \theta_1 - \sin^2 \theta_1) \quad (4)$$

$$R_{pp}(\theta_1) \approx A + B \sin^2 \theta_1 + C(\tan^2 \theta_1 - \sin^2 \theta_1) \quad (5)$$

$$\Delta\rho = \rho_2 - \rho_1 \quad (6)$$

$$\Delta Vp = Vp_2 - Vp_1 \quad (7)$$

$$\Delta\rho_a = (\rho_2 + \rho_1) / 2 \quad (8)$$

$$\Delta Vp_a = (Vp_1 + Vp_2) / 2 \quad (9)$$

$R_p = A$ (Reflection coefficient for normal incidence). Here, θ_1 denotes incidence angle, Vp is P-wave velocity, σ is Poisson ratio, and ρ is density at an interface. In practice, since the data is acquired up to 30 degree the third term of the Shuey's approach is eliminated. Thus, the Shuey's approach becomes:

$$R_{pp}(\theta_1) \approx A + B \sin^2 \theta_1 \quad (10)$$

A , the first term of the approach, is the reflection coefficient for normal incidence case named as "intercept" attribute. B , the second term of the approach, shows the dependence on incidence angle named as "gradient" attribute.

A gas reservoir can be detected using the intercept and gradient attributes. A technique called cross-plot could be a "background trend" for the wet sand or shale for the cases where basement rock exists. The points outside of this trend may point out the existence of gas.

The AVO anomalies obtained as a result of the modelling study are defined according to the classification proposed by Rutherford and Williams (1989). These authors classify the AVO anomalies into three groups namely class I, II and III to distinguish the gas and petroleum masses. In class I, the reflection coefficients are positive for normal incidence and the reflection coefficient values decrease with the increasing offsets. The acoustic impedance of the reservoir is larger than the upper layer's one. In class II, the reflection coefficients are close to zero and become negative with the increasing offsets. The acoustic impedance of the reservoir is close to the upper layer's one and a polarity reversal may appear. In class III, the reflection coefficients for normal incidence are negative and the negative value is getting larger with increasing offsets. The acoustic impedance of the reservoir is smaller than the upper layer's one.

Castagna and Swan (1997) proposed class IV AVO anomaly in addition to the three classes defined by Rutherford and Williams (1989). In their class IV AVO anomaly, the amplitudes are similar to the class III amplitudes, the reflection coefficients are negative but the absolute value of the amplitudes decrease with increasing offsets.

Data analysis

The velocity model

During the elaboration of the model given in Figure 1 the synthetic well log data is generated from the velocities attributed to different levels up to a depth of 2000 m beneath the points (CDP 1100-1200-1300) which are shown as vertical red lines along the upper part of the model. The correlation of thus generated synthetic well log data yields the geological model. After applying the required data processing to the synthetic seismic reflection data obtained from the shots on this model the AVO analysis is carried out. The shale layer is in the 200 to 250 m depth range, the horizontal gassy sand layers occur as 10 m thick layer at 1400 m depth, as 30 m thick layer at 1600 m depth level, and as 20 m thick layer at 1800 m depth level. The rest of the model includes clay-sand layer units. The model elaboration, the data processing and the AVO analysis applications were carried out at TPAO Data Processing Center using the ProMax software.

Synthetic records

In our model the spreading length was selected as 3000 m for each shot point and the calculations were done by using finite difference method. Source-receiver distance is 12.5 m, the total shot points is

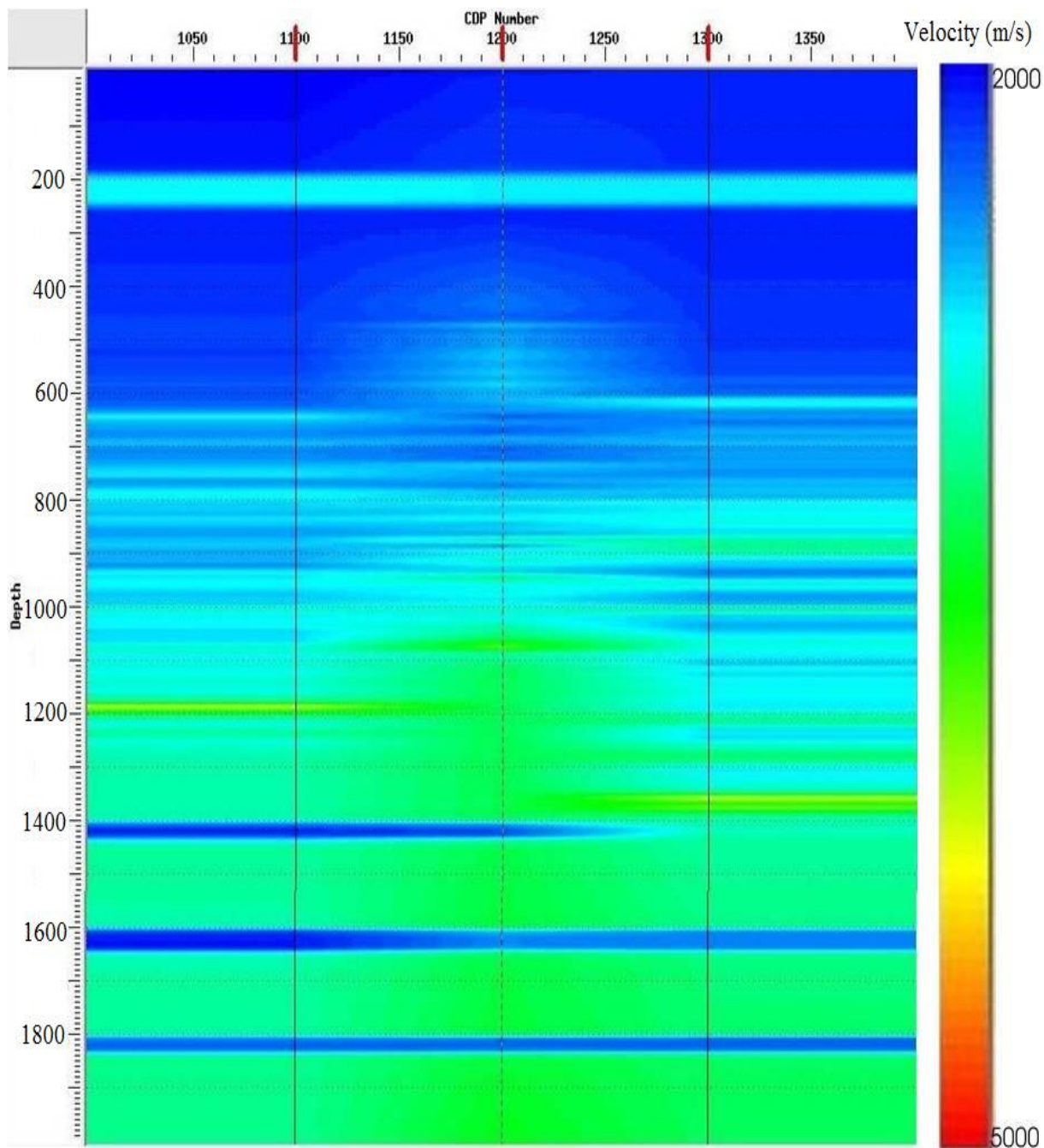


Figure 1. The velocity model. During the elaboration of the model the synthetic well log data is generated from the velocities attributed to different levels up to a depth of 2000 m beneath the points (CDP 1100-1200-1300) which are shown as vertical red lines along the upper part of the model. The correlation of thus generated synthetic well log data yields the geological model.

230, the receiver number is 240 and 60-fold CDP data were synthesized. The shooting interval was 50 m where the shot point spacing is 25 m. The data samples for the 1100-1200-1300 CDP trace gathers are given in Figure 2.

NMO, muting and stacking data processing were applied to the reflection data acquired from layers of different features. The layers pointed out with the capital letters A, B, C in the cross-section are the gassy sand layers given in the initial model (Figure 3).

AVO analysis

The intercept yields the best reflectivity cross-sections. Here, the reflectivity that includes gas are identified with the polarities. Figure 4 is the cross-section of intercept attribute. The gradient indicates amplitude variation ratio depending on an angle. Generally, although the amplitude variation dependence on an angle is not observed at other reflectors large amplitude variations are observed

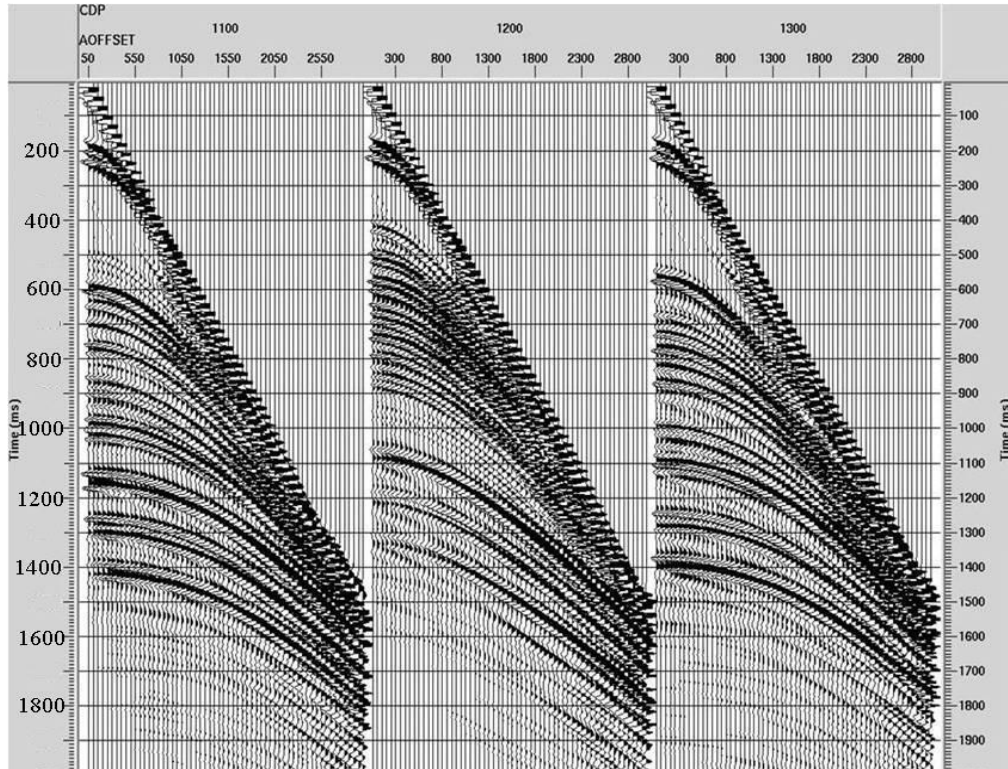


Figure 2. 60-fold CDP data samples for the 1100-1200-1300 CDP trace gathers. The spreading length was selected as 3000 m for each shot point. Source-receiver distance, the total shot points and receiver number were indicated as 12.5, 230 and 240 m, in respectively. The shooting interval is 50 m where the shot point spacing is 25 m.

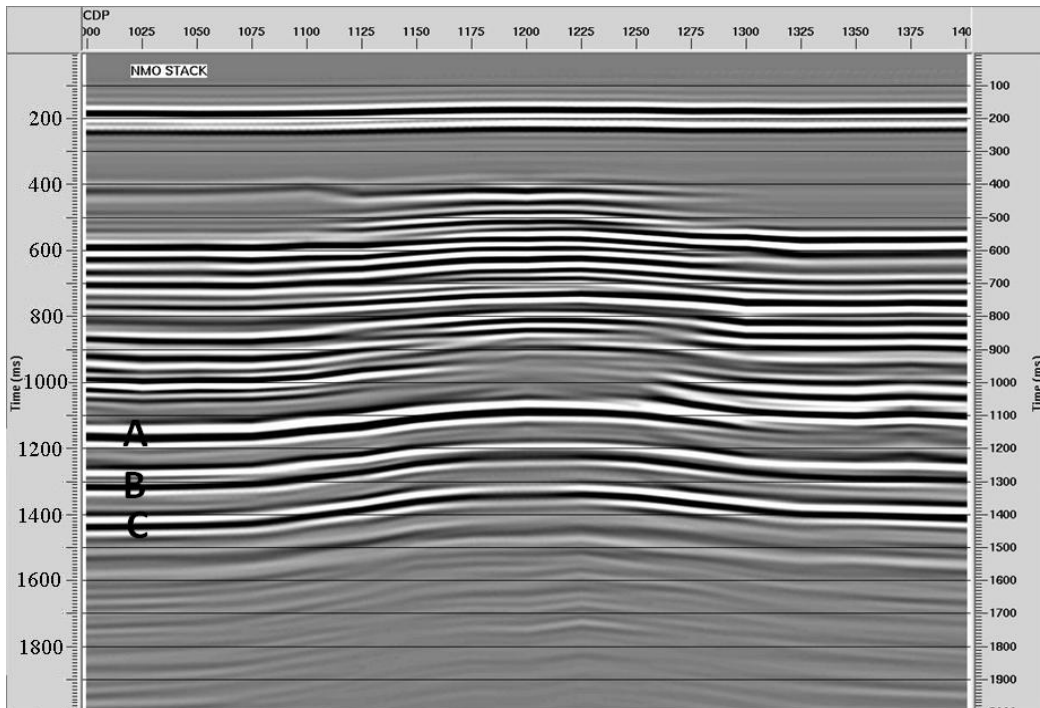


Figure 3. NMO stack section after Muting. The gassy sand layers given in the initial model pointed out with the capital letters A, B, C.

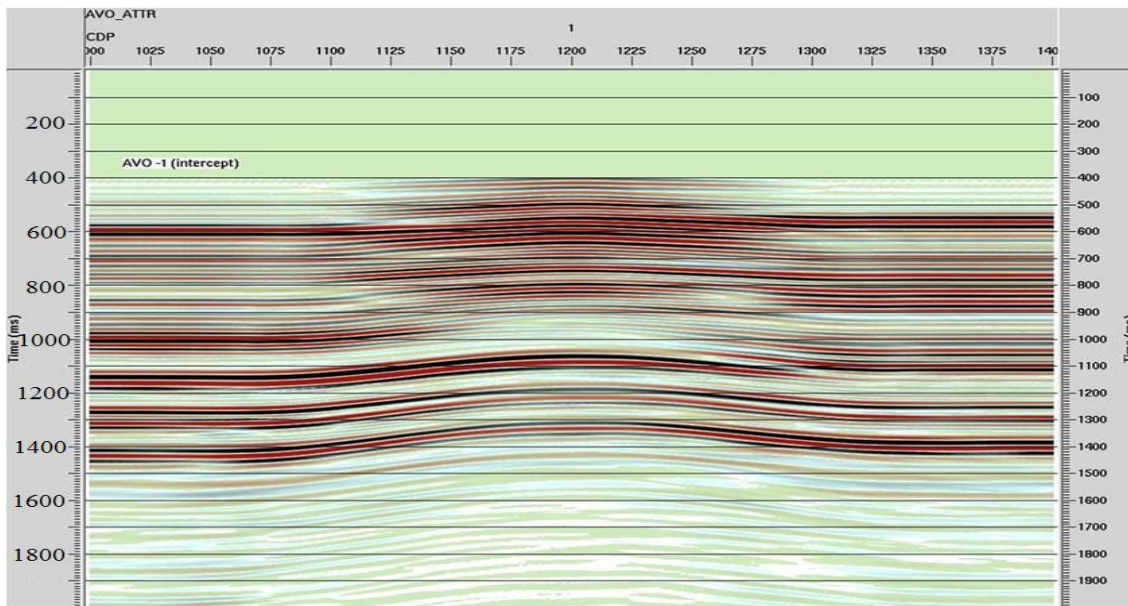


Figure 4. The cross-section of intercept attribute. The intercept yields the best reflectivity cross-sections. The reflectivity that includes gases are identified with the polarities.

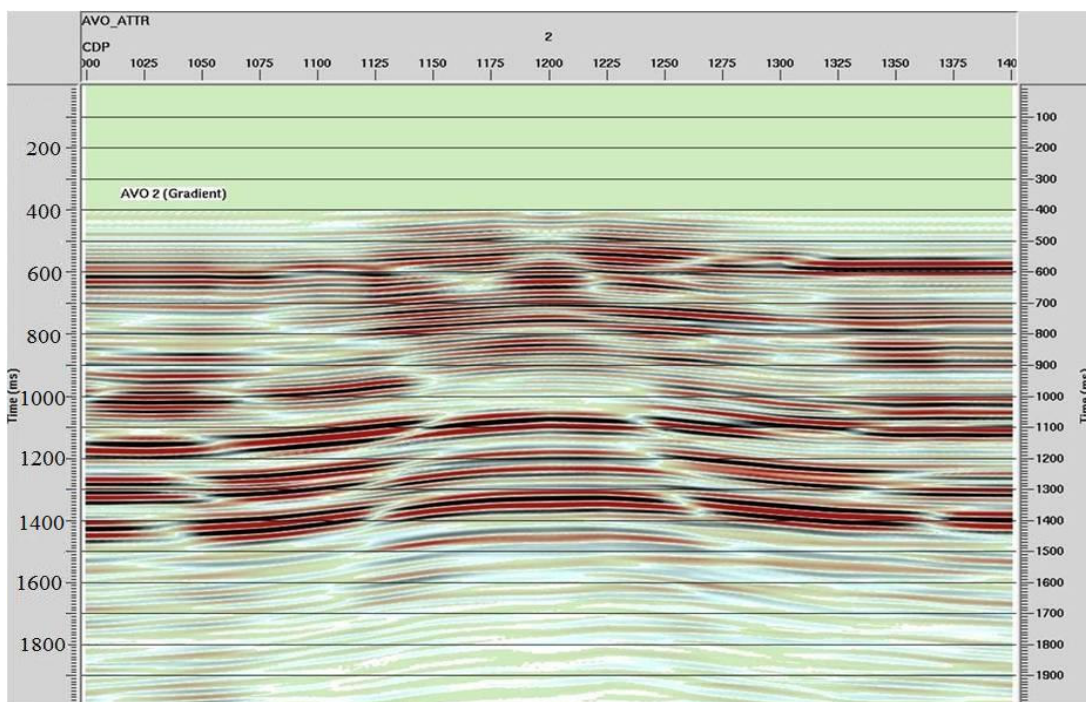


Figure 5. The cross-section of gradient attribute. This attribute indicates amplitude variation ratio depending on an angle. Generally, although the amplitude variation dependence on an angle is not observed at other reflectors large amplitude variations are observed at gassy sand reflectors.

at gassy sand reflectors (Figure 5).

Since the intercept displays the P wave reflectivity and the gradient shows the amplitude variations depending on an angle the intercept* gradient which is the product of the two attributes

indicates both the polarity and the angle dependence of the amplitude variations. The red color identified with this attribute correlates well with the gas anomaly determined from the other attributes (Figure 6).

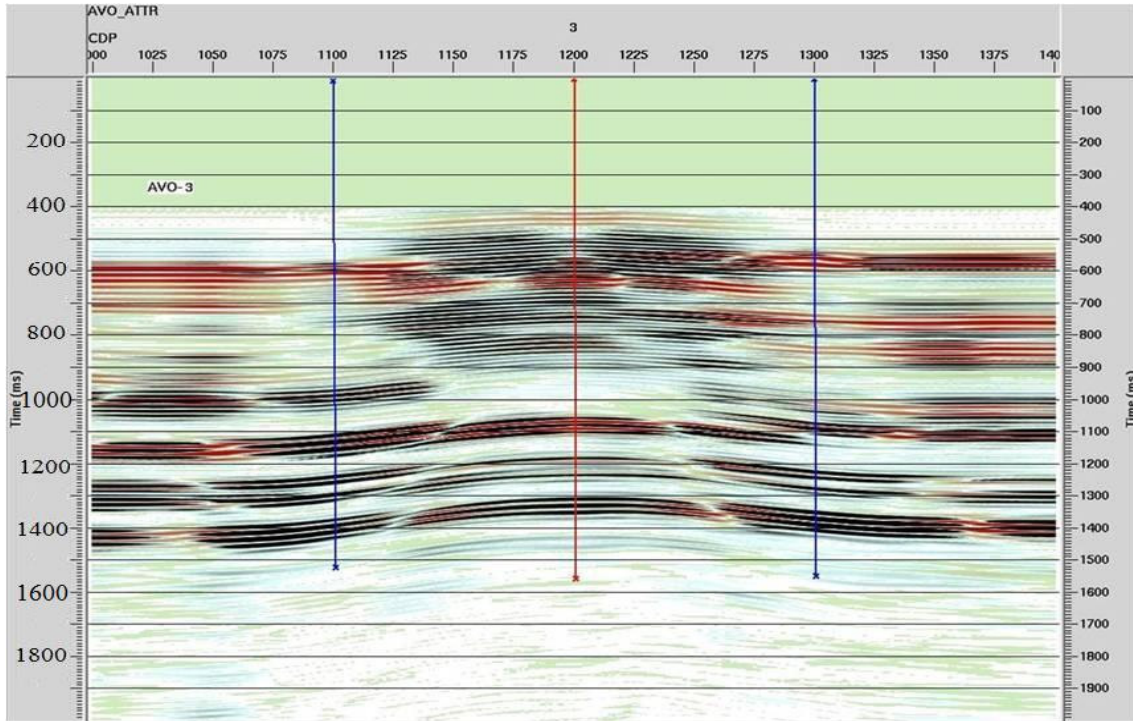


Figure 6. The cross-section of intercept*gradient attribute. The intercept* gradient which is the product of the two attributes indicates both the polarity and the angle dependence of the amplitude variations. The red color identified with this attribute correlates well with the gas anomaly determined from the other attributes.

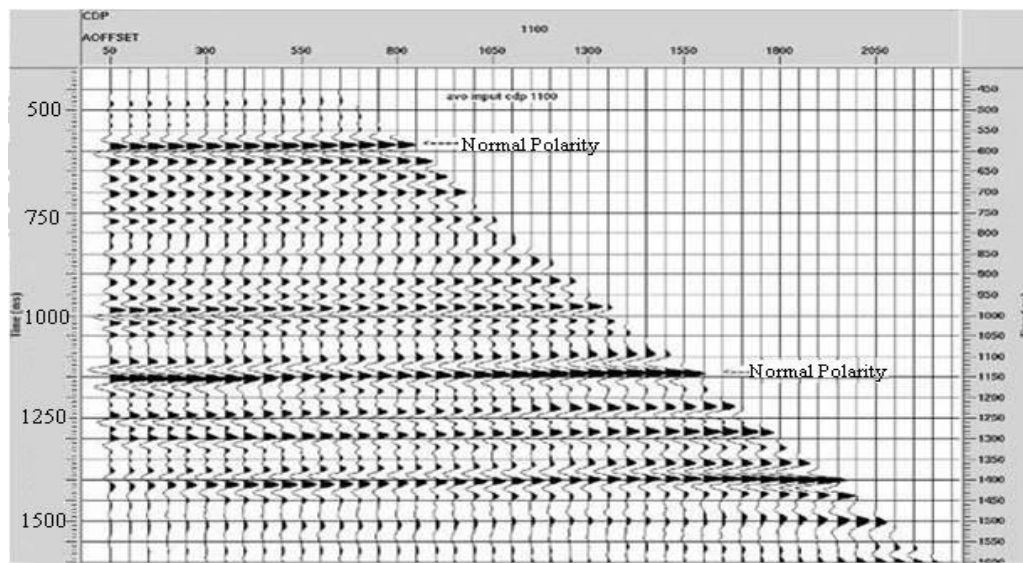


Figure 7. The cross-section of intercept* gradient attribute of the 1100 CDP trace gathers.

Common depth point (CDP) trace gathers

All the AVO attributes should be taken into account when the interpretation is carried out through AVO analysis. The CDP trace gathers are used to check the stacked AVO attribute cross-sections (Figures 7, 8, and 9).

Crossplot

Our results show that the gassy sand layers yield class III AVO anomaly. That is to say, the amplitude increases with the increasing offsets. The AVO anomaly in the CDP 1300 trace gather is not so much strong as the one observed at the CDP 1100 and CDP 1200

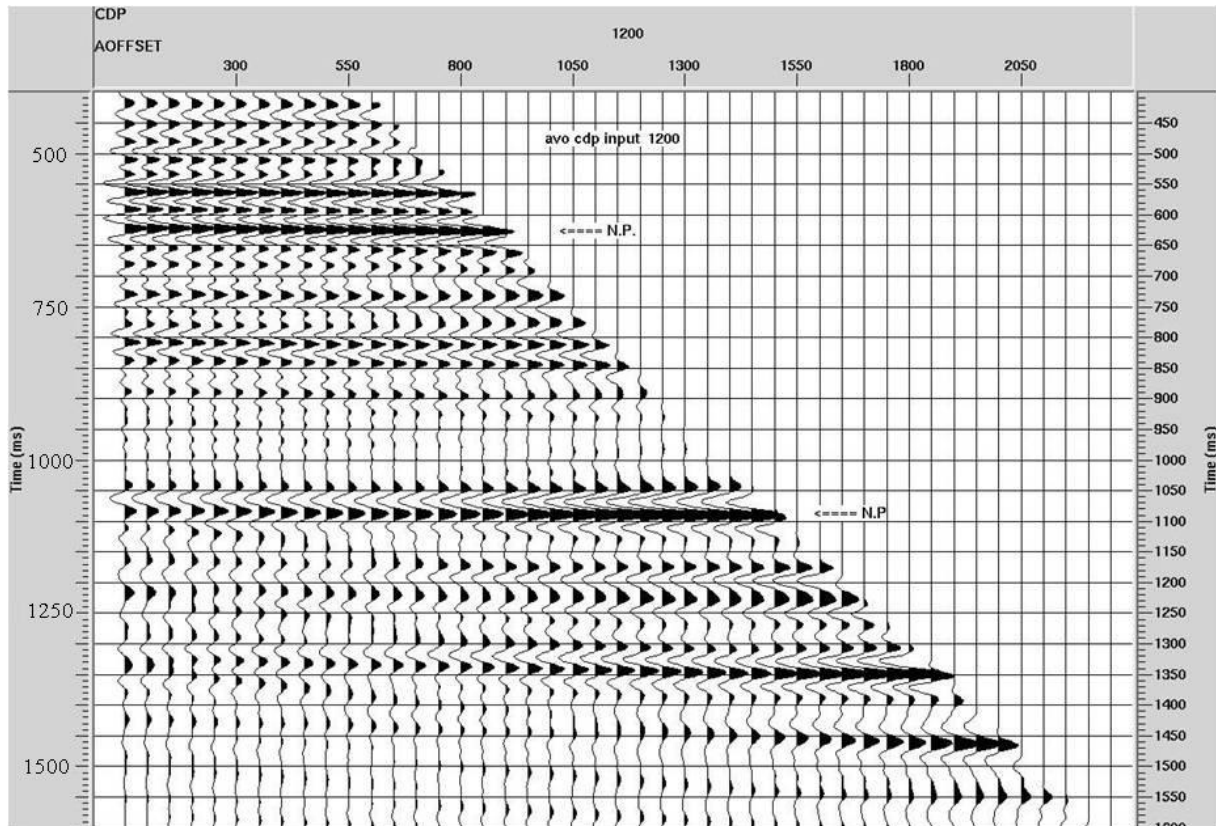


Figure 8. The cross-section of intercept* gradient attribute of the 1200 CDP trace gathers.

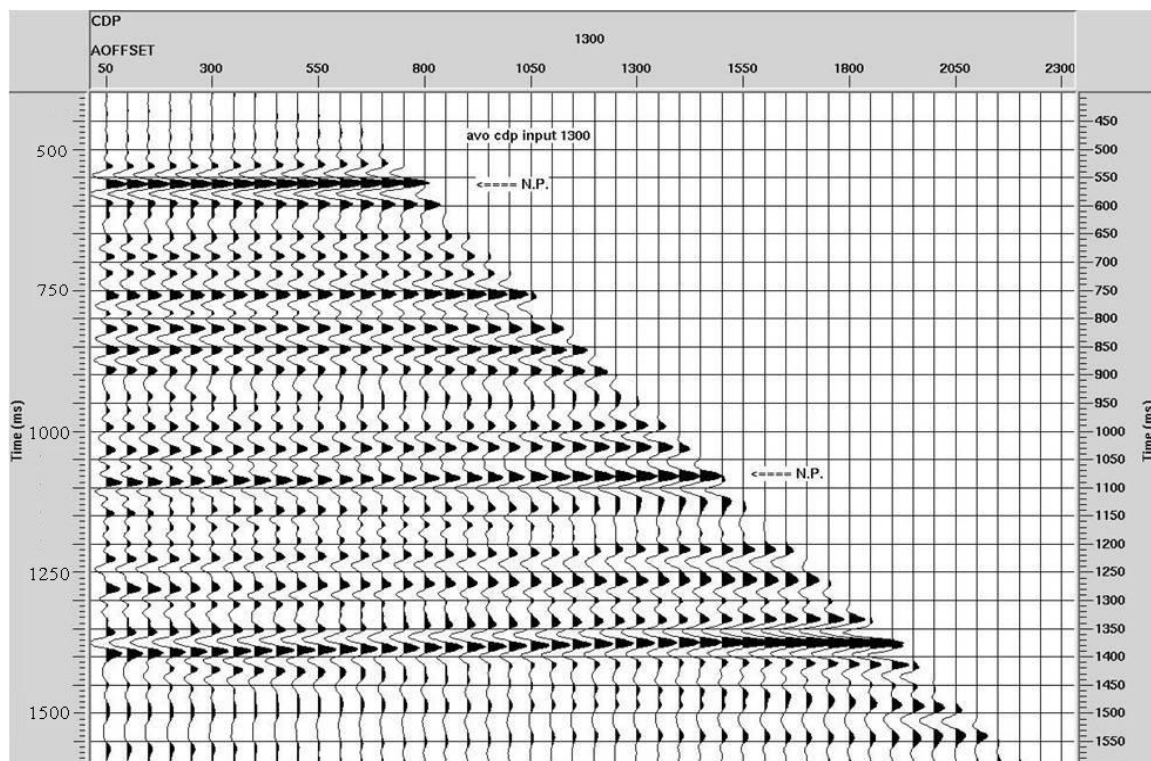


Figure 9. The cross-section of intercept* gradient attribute of the 1300 CDP trace gathers.

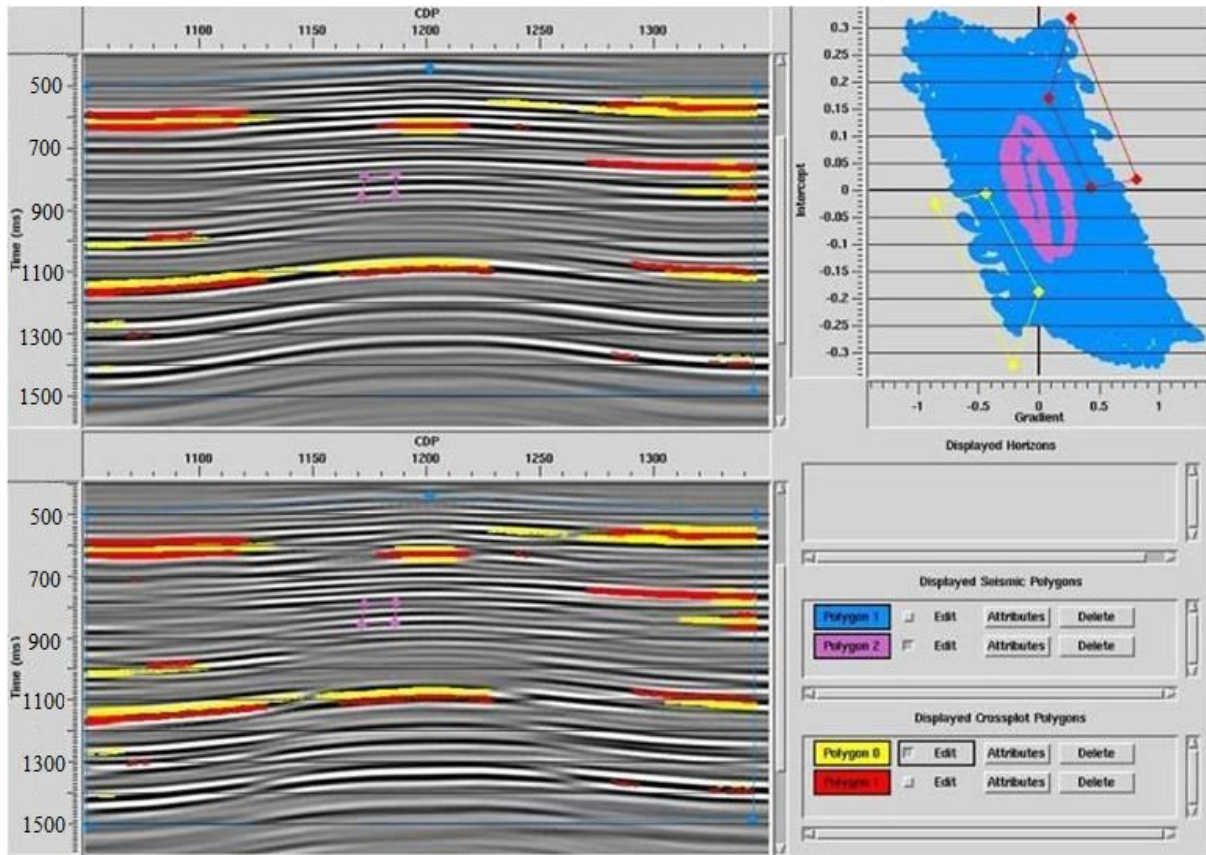


Figure 10. Crossplot section shows that the gassy sand layers yield class III AVO anomaly. So the amplitude increases with the increasing offsets.

trace gathers (Figure 10).

RESULTS AND DISCUSSION

As a result of the AVO analysis the intercept, gradient, intercept* gradient attribute cross-sections were derived. We use the 1100-1200-1300 CDP trace gathers where well logs info exists to check the stacked AVO attribute cross-sections. As observed in the CDP trace gather cross-sections class III AVO anomaly is observed at gassy sand levels. Since the gassy sand levels disappear at the 1300 CDP trace gather no AVO anomaly similar to the CDP 1100 and CDP 1200 trace gathers were detected. Despite the lack of gassy sand at some levels AVO anomaly was observed at the cross-plot of the intercept and gradient attributes. Although the layers in the geological model are horizontal, these layers might gently dip in the cross-sections. This might be because of velocity traction resulting from the large velocity of the upper layer. This effect can be eliminated only at depth domain. However, since our study is in time domain we have not eliminated the foregoing effect. For this reason, no AVO anomalies were observed at levels where no

gassy sand exists. Consequently, all the AVO attributes should be taken into account for a robust AVO analysis. Also, because some kind of errors or lack of data processing stages during AVO analysis would affect the results the interpreter should take special care for such instances.

Nonetheless, the data processing stages depends on the data itself. Particularly, for the locations where the tectonics and folding is active advanced data processing tools is a must. The success rate depends on whether the analysis methods and algorithms are tailored according to the needs of the site under investigation. Despite some drawbacks the method plays an important role in determination of reservoir characteristics during hydrocarbon exploration, development and production.

ACKNOWLEDGEMENTS

The authors appreciate the contributions made by Ayhan Özkan and Zafer Özer and the head of the Exploration Division who arranged and allowed to benefit from the facilities of TPAO.

REFERENCES

- Aki K, Richards PG (1980). Quantitative seismology theory and methods. V. I-II, W. H. and Co.
- Bortfeld R (1961). Approximation to the reflection and transmission coefficients of plane longitudinal and transverse waves. *Geophys. Prosp.*, 9: 485-503.
- Castagna JP, Swan W (1997). Principles of AVO crossplotting. *Lead. Edge*, 16: 337-342.
- Chiburis EF (1984). Analysis of amplitude versus offset to detect gas-oil contacts in Arabian Gulf. 54th Ann. Int. Mtg. Soc. Expl. Geophys., pp. 669-670.
- Çiftçi C (2008). Açılıma bağlı reflektivite analizi. Yüksek lisans tezi, Süleyman Demirel Üniversitesi, Fen Bilimleri Enstitüsü, Isparta, Türkiye (in Turkish with English abstract).
- Çiftçi C, Özer Z, Kamacı Z (2009). Hidrokarbon Aramacılığında Bir Sayısal Jeolojik Modelin Açılıma Bağlı Reflektivite (AVO) Analizi. 62. Jeoloji Kurultayı 13-17 Nisan, Ankara, pp. 564-565 (in Turkish).
- Knott CG (1899). Reflection and refraction of elastic waves with seismological applications. *Phil. Mag.*, 48: 64-97.
- Ostrander WJ (1984). Plane wave reflection coefficients for gas sands at non-normal angles of incidence. *Geophys.*, 49: 1637-1648.
- Richards PG, Frasier, CW (1976). Scattering of elastic waves from depth dependent inhomogeneities. *Geophys.*, 41: 441-458.
- Rutherford SR, Williams RH (1989). Amplitude versus offset variations in gas sands. *Geophys.*, 54: 680-688.
- Sandıkçı E (2010). Hazne kayadaki gaz, su ve çözünmüş gaz içeren suyun AVA ve LMR analizleri ile ayırt edilmesi. Türkiye 19. Uluslararası Jeofizik Kongre ve Sergisi, Ankara, Türkiye (in Turkish with English abstract).
- Shuey RT (1985). A Simplification of the Zoeppritz equations. *Geophysics*, 50: 609-614.
- Sincer İ (2008). Sismik yansıma yönteminin esasları ve uygulamaları. TPAO, Ankara, p. 175 (in Turkish).
- Todd CP (1986). Isolation, display and interpretation of offset dependent phenomena in seismic reflection data using offset to depth range partial stacking. M.Sc. Thesis. Univ. Texas, Houston.
- Yavuz S, Demirbağ E (2010). Batı Karadeniz'de gaz hidrat anomalilerinin AVO analizi ile incelenmesi. Türkiye 19. Uluslararası Jeofizik Kongre ve Sergisi, Ankara, Türkiye (in Turkish with English abstract).
- Yu G (1985). Offset amplitude variation and controlled amplitude processing. 55th Ann. Int. Mtg. Soc. Expl. Geophys. Expanded Abstracts, pp. 591-594.
- Zoeppritz K (1919). On the reflection and propagation of seismic waves. *Göttinger Nachrichten*, 1: 66-84.